Publications of the Korean Astronomical Society
32: 163 ∼ 167, 2017 March

pISSN 1225-1534
eISSN 2287-6936
https://doi.org/10.5303/PKAS.2017.32.1.163

AKARI SPECTROSCOPY OF QUASARS AT 2.5 – 5 MICRON

Myungshin Im[1], Hyunsung Jun[1,2], Dohyeong Kim[1], Hyung Mok Lee[1], Youichi Ohyama[3], Ji Hoon Kim[1,4], Takao Nakagawa[5], and QSONG Team[1,2,3,4,5]

[1]CEOU/Astronomy Program, Department of Physics & Astronomy, 1 Kwanak-rho, Kwanak-gu, Seoul 151-742, Korea
[2]Jet Propulsion Laboratory, California Institute of Technology, 4800 Oak Grove Drive, Pasadena, CA 91109, USA
[3]Academia Sinica, Institute of Astronomy & Astrophysics, P.O. Box 23-141, Taipei 10617, Taiwan, China
[4]Subaru Telescope, National Astronomical Observatory of Japan, 650 N. A'ohoku Place, Hilo, Hawaii, HI 96720, USA
[5]Institute of Space and Astronautical Science, JAXA, Sagamihara, Kanagawa, 252-5120, Japan

E-mail: mim@astro.snu.ac.kr

(Received February 20, 2016; Revised October 15, 2016; Accepted October 15, 2016)

ABSTRACT

Utilizing a unique capability of *AKARI* that allows deep spectroscopy at 2.5 – 5.0 μm, we performed a spectroscopy study of more than 200 quasars through one of the *AKARI* mission programs, QSONG (Quasar Spectroscopic Observation with NIR Grism). QSONG targeted 155 high redshift ($3.3 < z < 6.42$) quasars and 90 low redshift active galactic nuclei ($0.002 < z < 0.48$). In order to provide black hole mass estimates based on the rest-frame optical spectra, the high redshift part of QSONG is designed to detect the Hα line and the rest-frame optical spectra of quasars at $z > 3.3$. The low redshift part of QSONG is geared to uncover the rest-frame 2.5 – 5.0 μm spectral features of active galactic nuclei to gain useful information such as the dust-extinction-free black hole mass estimators based on the Brackett lines and the temperatures of the hot dust torus. We outline the program strategy, and present some of the scientific highlights from QSONG, including the detection of the Hα line from a quasar at $z > 4.5$ which indicates a rigorous growth of black holes in the early universe, and the Brβ-based black hole mass estimators and the hot dust temperatures ($\sim$ 1100 K) of low redshift AGNs.

Key words: infrared: galaxies — galaxies: active — galaxies: nuclei

1. INTRODUCTION

Supermassive black holes (SMBHs) are black holes with masses of order of 10^6 – $10^{10}\,M_\odot$. They are known to exist at the center of spheroidal components of galaxies such as bulge of spiral galaxies and elliptical galaxies. SMBHs in active accretion phase power active galactic nuclei (AGNs) and quasars whose powerful radiation outshine their host galaxies. Quasars and AGNs are now identified as far back as to the epoch of reionization, with the currently known highest redshift quasar at $z \sim 7$ (Mortlock et al., 2011). Interestingly, the black hole mass ($M_{\rm BH}$) of quasars at $z > 6$ suggest that they are as massive as $M \sim 10^9\,M_\odot$. In other words, a few billion $M_\odot$ SMBHs were already in place when the universe was less than 1 Gyr old, and growing stellar mass black holes to SMBHs is not a simple task in such a time scale (e.g., see Natarajan, 2014).

To study the growth of SMBHs, it is critical to estimate $M_{\rm BH}$ reliably. So far, $M_{\rm BH}$ of high redshift quasars have been measured using UV emission lines such as C IV or Mg II, but the reliability of such mass indicators is in debate. In particular the C IV-based mass estimator has been found to have a large dispersion in comparison to MgII or Balmer line based mass estimators (e.g., Netzer et al., 2007). Other systematic effects such as the metallicity dependence of the relation are not well explored, but could influence the mass estimates if strong metallicity evolution exists at high redshift. One way to overcome these problems is to utilize the hydrogen Balmer lines to measure $M_{\rm BH}$s. Being independent of

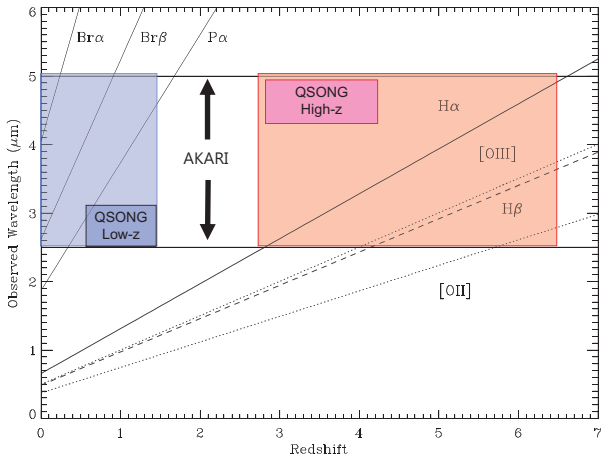

Figure 1. The observed wavelengths of the hydrogen and other atomic lines as a function of redshift. At $z > 3 - 4$, the prominent hydrogen lines such as Hα and Hβ redshift into the *AKARI*'s unique spectroscopic wavelength window of 2.5 – 5.0 μm which sits between the K-band of the ground-based telescopes and the *Spitzer* IRS coverage. *AKARI* is currently the only facility which was capable to detect these lines from faint sources such as quasars. The high redshift part of the QSONG program focuses on these key wavelength regions, while the low redshift part of the QSONG program aims to detect NIR hydrogen lines such as Brα, Brβ, and Pα of nearby type-1 AGNs to construct mass estimators that are less affected by dust extinction (e.g., Kim et al., 2010, 2015).

nucleosynthesis, the hydrogen abundance is not affected by the metallicity evolution. Also, the hydrogen-based mass estimators are more directly tied to the reverberation mapping-based mass estimators than the UV line-based estimators, thus are more fundamental than the UV line-based estimators.

Another interesting question in AGN study involves the study of AGN in very active phase. In some models, SMBHs are born at the center of dusty starburst galaxies, and the early growth of SMBHs involve red, dusty AGN phase. To test such a scenario, it is imperative to measure $M_{\rm BH}$, but such a task is difficult with the $M_{\rm BH}$ estimators using the rest-frame optical or UV spectra since they are prone to the dust extinction. One can alleviate the problem with the dust extinction by using $M_{\rm BH}$ mass estimators based on the NIR hydrogen Paschen line (Kim et al., 2010). The extension of the method to a longer wavelength line such as the Brackett lines would help investigate the nature of AGNs in the dust-enshrouded phase.

However, there exists a practical difficulty in using the Balmer lines of high redshift quasars or the Brackett lines of low redshift AGNs to determine $M_{\rm BH}$s. Figure 1 shows how the observed wavelengths of the Balmer and the Brackett lines change as a function of redshift. At $z > 3$–4, the observed wavelengths of the Hα and Hβ lines redshift into the wavelength of 2.5–5.0 μm, which is practically impossible to reach from the ground for faint objects like distant quasars, and out of the spectral coverage from the *Spitzer*.

The *AKARI*'s unique wavelength coverage at 2.5–5.0 μm, coupled with a very low sky background in the space at this wavelength window, enables us to detect the redshifted Hα line as far as $z = 6.4$ and the Brα or Brβ lines at low redshift. Hence, we performed *AKARI* open time programs, and an AKARI mission program, Quasars Spectroscopic Observation in NIR Grism (QSONG; PI: Lee, H. M.), to understand the growth of SMBHs at high and low redshifts. Here, we give an overview of these programs, and present preliminary results, including the first detection of the Hα lines at $z > 4.5$.

2. OVERVIEW OF QSONG

The observations of high redshift quasars were carried out both during the phase 2 (cold phase) and the phase 3 (warm phase) periods as open time programs, HZQSO, HQSO2, DPQSO (PI: M. Im), and a mission program, QSONG. Here, we describe each program.

The HZQSO can be considered as a pilot program of QSONG. It was carried out during the phase 2 period, and the main objective of HZQSO was to unveil the redshifted optical spectra of distant quasars at $4.5 < z < 6.43$. The targets for the HZQSO program were selected from a list of quasars at $z > 4.5$ that were known when the proposal was written (2006). The list of quasars includes those from the APM-UKST survey (Storrie-Lombardi et al., 1996) and the Sloan Digital Sky Survey (SDSS) quasars.

The observation was performed during 2006 – 2007, with the NIR grism (NG) or prism (NP) mode of IRC (Onaka et al., 2007). The data for 12 targets were obtained. The NG mode provides a spectral resolution of $R \sim 120$, which is ideal for detecting strong broad emission lines of quasars (typical FWHM of 4000 km s^{-1}). The NP mode offers a higher throughput but a lower spectral resolution than the NG mode. For some targets, both NP and NG data were taken so that we can determine the continuum level of the object better. For some other targets, only prism data were taken since the number of available observing opportunities was limited.

Motivated by the success of the HZQSO observations, QSONG was performed during the post-He cool-

Table 1
QSONG Sample

Redshift	Number	$\log(L_{\rm bol}/L_\odot)$	$\log(M/M_\odot)$
$3.3 < z < 6.43$	155	$\gtrsim 47$	$\gtrsim 9$
$0.002 < z < 0.48$	90	43.1 – 47.2	6.3 – 9.7

ing phase as a mission program using the NG mode. In comparison to the HZQSO program, the target selection was broadened to include quasars at $3.4 < z < 6.4$, and the number of targets was increased to more than 200. For quasars at $z < 5.5$, a magnitude limit was set at $z \lesssim 19$ mag with the on-source integration times of 400 – 2000 secs. These limits roughly correspond to a bolometric luminosity limit of $L_{\rm bol} \gtrsim 10^{47}{\rm ergs}^{-1}$, and a $M_{\rm BH}$ limit of $M > 10^9 M_\odot$. The open time programs HQSO2 and DPQSO (PI: M. Im) were carried out to complement QSONG, by observing fainter objects ($z \lesssim 20$ mag) at higher redshifts ($z > 5.5$) with longer exposure times. Overall, the reduced sensitivity and the increased number of hot pixels of IRC in the warm phase made it challenging to accumulate enough S/N, compared to the HZQSO program.

In QSONG, we also targeted low redshift type-1 AGNs, red AGNs and AGNs at low galactic latitude (Lee et al., 2008; Im et al., 2007). The main scientific purposes of the low redshift QSONG program are to (i) establish $M_{\rm BH}$ estimators based on the Brα, and Brβ lines; (ii) use the NIR $M_{\rm BH}$ estimators to derive SMBH masses of red quasars; (iii) investigate the 3.3 μm PAH feature of nearby AGN as a means to understand the star formation occurring in their host galaxies (e.g., Kim et al., 2012; Yamada et al., 2013); and (iv) derive AGN hot dust temperatures. Since the NIR hydrogen lines are much less affected by dust extinction than the optical/UV emission lines that are commonly used for estimating $M_{\rm BH}$, establishing black hole mass estimators with NIR hydrogen lines has an obvious application to dust-reddened AGNs. Therefore, red AGNs and low galactic latitude AGNs – both of which are affected by dust extinction – are included in order to apply the NIR-based $M_{\rm BH}$ estimators to the dust-reddened AGNs (e.g., Kim et al., 2010). Overall, we observed 90 nearby type-1 AGNs with the NG mode, most of which are PG quasars or AGNs studied by the reverberation mapping. Twelve red AGNs were observed too. The observation method was similar to the high redshift QSONG program.

Table 1 summarize the number of targets and their properties.

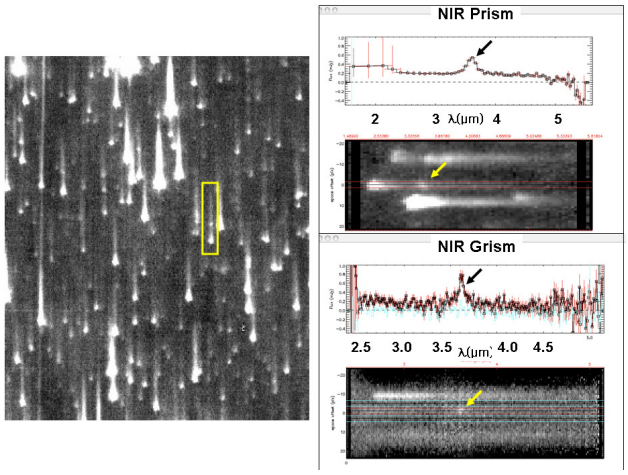

Figure 2. (Left) The slitless *AKARI* NP spectroscopy image taken of the field around BR 0006-6224 at $z = 4.51$. The figure shows the spectra of many sources, with the spectrum of the quasar marked with a rectangular box. There are a continuum and a redshifted Hα line appearing as a bright spot on the spectrum; (Right) The extracted 1-D and 2-D NP spectrum of BR0006-6224 (top), and the 1-D and 2-D NG spectrum of the same object which shows the resolved Hα line observed at 3.6 μm (indicated by an arrow).

3. SCIENCE HIGHLIGHTS

3.1. Detection of Hα at $z > 4.5$

Figure 2 shows an example of the Hα line detected at high redshift. It shows a NP slitless spectroscopy image (left), and the extracted NP and NG spectra of BR 0006-6224 at $z = 4.51$ (right). The tadpole-like features in the spectroscopy image are the spectra of the sources in the field of BR 0006-6224, with the head part of the tadpole-shaped spectrum indicating the shorter wavelength. The location of the BR 0006-6224 spectrum is marked with a rectangular box, and a bright spot in the middle of the spectrum is the redshifted Hα line. The extracted NP and NG, 1-D and 2-D spectra of BR 0006-6224 (right) show a strong detection of the redshifted Hα line at 3.6 μm. This marks the first detection of the redshifted Hα line at $z > 4.5$, superseding the previous record of $z = 4.3$ (Oyabu et al., 2007; Sedgwick et al., 2013).

The Hα lines were detected in 72 quasars in the NG mode at $S/N > 2$, and they were fitted with a single Gaussian profile (due to the low spectral resolution) to derive their line widths and luminosities, and eventually $M_{\rm BH}$s. The derived $M_{\rm BH}$ values show a good agreement with the Mg II-based $M_{\rm BH}$ values, but a large scatter is

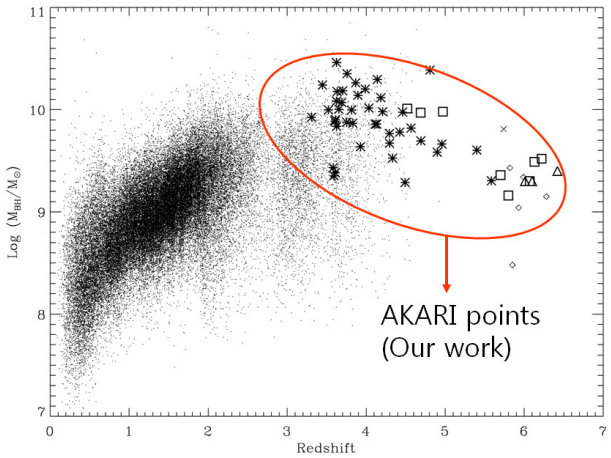

Figure 3. The redshift versus $M_{\rm BH}$ in AGNs. The $M_{\rm BH}$ values derived from the Hα line are marked with the thick points (different symbols indicate results from different programs), and the small dots show the $M_{\rm BH}$ values from Shen et al. (2008) where $M_{\rm BH}$s of high redshift quasars mostly come from C IV.

found in comparison to the C IV-based $M_{\rm BH}$ estimates.

Figure 3 shows a preliminary result showing the redshift versus $M_{\rm BH}$ of the QSONG quasars over-plotted on the SDSS quasars from Shen et al. (2008). We confirm that quasars with $M_{\rm BH}$s of a few billion $M_\odot$ exist out to $z \sim 6$, and even quasars with extremely massive black holes (EMBHs) with $M_{\rm BH} \sim 10^{10}\,M_\odot$ exist out to $z \sim 5$. On the other hand, there seems to be a lack of EMBH quasars at $z \sim 6$. This result, together with the fact that $z \sim 6$ quasars are nearly in the Eddington limited accretion and hot-dust poor (e.g., Jiang et al., 2010; Jun & Im, 2013), suggests that we are witnessing the emergence of the most massive black holes at $z \sim 6$. More details of these results can be found in Jun et al. (2015).

3.2. *Brackett Lines and Hot Dust Temperature of Nearby AGNs*

Figure 4 shows an example of the *AKARI* spectrum of Mrk 110 at $z = 0.035$. In the spectrum, we see the detection of the Brα and Brβ lines as well as the 3.3 μm PAH feature.

The *AKARI* spectra similar to the one in Figure 4 are used to derive the Brackett line luminosities and widths of nearby AGNs. For the case of Brβ, there are six objects with S/N good enough to be used to derive a $M_{\rm BH}$ estimator. The Brackett line luminosities and widths are compared with the $M_{\rm BH}$ from the reverberation mapping method in the literature, and we find,

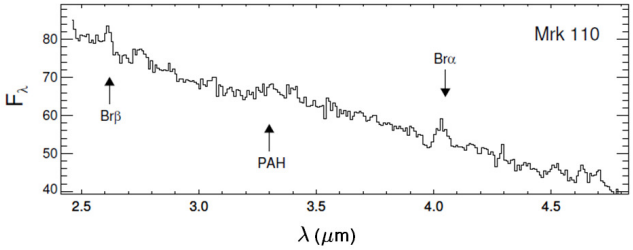

Figure 4. The 2.5 – 5.0 μm spectrum of Mrk 110. The Brα, Brβ, and PAH 3.3μm lines can be seen in the spectrum (from Kim et al., 2015).

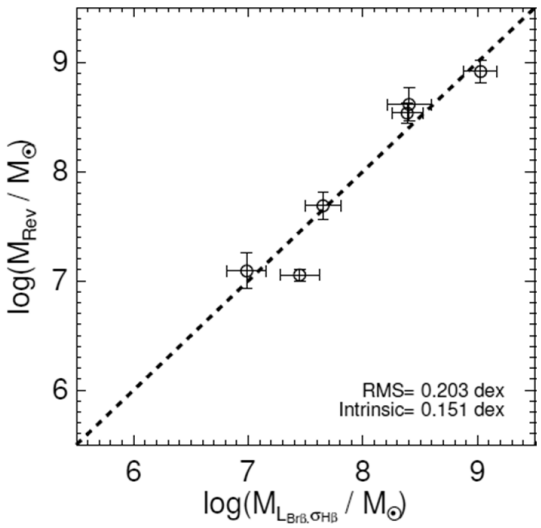

Figure 5. The comparison of the $M_{\rm BH}$ derived from the Brβ line versus $M_{\rm BH}$s of nearby AGNs from the reverberation mapping. The Brβ $M_{\rm BH}$ are derived using Eq. (1), and we find that the Brβ line can be used to estimate $M_{\rm BH}$ at an intrinsic scatter of ∼0.15 dex (from Kim et al., 2015).

$$\frac{M_{\rm BH}}{M_\odot} = 10^{5.92} \times \left(\frac{L_{\rm Br\beta}}{10^{42}\,{\rm erg\,s^{-1}}}\right)^{0.67} \left(\frac{\sigma_{\rm Br\beta}}{10^{3}\,{\rm km\,s^{-1}}}\right)^{2}, \quad (1)$$

with an intrinsic rms dispersion of $\sim$ 0.15 dex. Fig. 5 shows the Brβ $M_{\rm BH}$ estimator can provide a reliable $M_{\rm BH}$ estimates over a mass range of 10^7 to 10^9 $M_\odot$, which could be quite useful when studying obscured AGNs.

We also measured the dust temperature of the hot dust torus ($T_{\rm HD}$) of PG quasars, by fitting their continuum with a model made of a power law + double black body spectra for the hot and the warm dust temperatures. Thanks to the *AKARI* spectra that extend to 5 μm, we are able to provide a good measure of T_{HD}. Interestingly, as shown in Figure 6, the $T_{\rm HD}$ values are found to be about 1100 K on average, which is smaller than a commonly cited value of $T_{\rm HD} \sim 1500$ K (see also Oyabu et al., 2014).

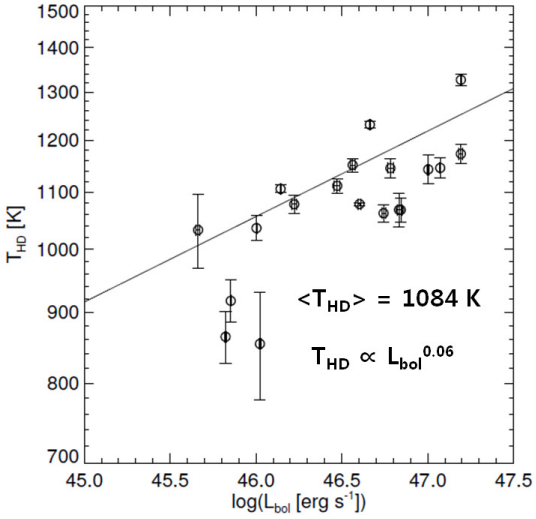

Figure 6. The $L_{\rm bol}$ versus $T_{\rm HD}$ of PG quasars. The derived $T_{\rm HD}$ values are much less than often cited values of $T_{\rm HD} \sim$ 1500 K (the figure is taken and modified from Kim et al., 2015).

These and other results, as well as the *AKARI* spectra of the QSONG low redshift sample are presented in Kim et al. (2014).

4. SUMMARY

We carried out a 2.5 - 5 μm spectroscopy of 155 high redshift quasars and 90 low redshift AGNs using *AKARI* IRC. Our study identified Hα lines of the high redshift quasars at $z > 4.5$ for the first time, which confirms the previous estimates of $M_{\rm BH}$ in high redshift quasars and reveals an active formation of SMBHs at high redshift. We also derived $M_{\rm BH}$ estimators based on the Brackett lines and found $T_{\rm HD} \sim 1100$ K for low redshift AGNs.

ACKNOWLEDGMENTS

We thank the members of the QSONG program for their contribution. This work was supported by the National Research Foundation of Korea (NRF) grant, No. 2008-0060544, funded by the Korea government (MSIP). This research is based on observations with AKARI, a JAXA project with the participation of ESA.

REFERENCES

Im, M., Lee, I., Cho, Y., et al., 2007, Seoul National University Bright Quasar Survey in Optical (SNUQSO). II. Discovery of 40 Bright Quasars Near the Galactic Plane, ApJ, 664, 64

Jiang, L., Fan, X., Brandt, W. N., et al., 2010, Dust-free quasars in the early Universe, Nature, 464, 380

Jun, H. D., Im, M., Lee, H. M., et al., 2015, Rest-frame Optical Spectra and Black Hole Masses of $3 < z < 6$ Quasars, ApJ, 806, 109

Jun, H. D. & Im, M., 2013, Physical Properties of Luminous Dust-poor Quasars, ApJ, 779, 104

Kim, D., Im, M., Kim, J. H., et al., 2015, The AKARI 2.5-5.0 μm Spectral Atlas of Type-1 Active Galactic Nuclei: Black Hole Mass Estimator, Line Ratio, and Hot Dust Temperature, ApJS, 216, 17

Kim, J., Im, M., Lee, H. M., et al., 2012, The 3.3 μm Polycyclic Aromatic Hydrocarbon Emission as a Star Formation Rate Indicator, ApJ, 760, 120

Lee, I., Im, M., Kim, M., et al., 2008, Seoul National University Bright Quasar Survey in Optical (SNUQSO). I. First Phase Observations and Results, ApJS, 175, 116

Mortlock, D. J., Warren, S. J., Venemans, B. P., et al., 2011, A luminous quasar at a redshift of $z = 7.085$, Nature, 474, 616

Natarajan, P., 2014, Seeds to monsters: tracing the growth of black holes in the universe, Gen. Rel. and Grav., 46, 1702

Netzer, H., Lira, P., Trakhtenbrot, B., Schemmer, O., & Cury, I., 2007, Black Hole Mass and Growth Rate at High Redshift, ApJ, 671, 1256

Onaka, T., Matsuhara, H., Wada, T., et al., 2007,The Infrared Camera (IRC) for AKARI – Design and Imaging Performance, PASJ, 59S, 401

Oyabu, S., et al., 2014, in this proceedings

Oyabu, S., Wada, T., Ohyama, Y., et al., 2007, Detection of an Hα Emission Line on a Quasar, RX J1759.4+6638, at $z = 4.3$ with AKARI, PASJ, 59, 497

Sedgwick, C., Serjeant, S., Pearson, C., et al., 2013, Detection of Hα emission from $z > 3.5$ submillimetre luminous galaxies with AKARI-FUHYU spectroscopy, MNRAS, 436, 395

Shen, Y., Greene, J. E., Strauss, M. A., et al., 2008, Biases in Virial Black Hole Masses: An SDSS Perspective, ApJ, 680, 169

Storrie-Lombardi, L. J., McMahon, R. G., Irwin, M. J., & Hazard, C., 1996, APM $Z \geq 4$ QSO Survey: Spectra and Intervening Absorption Systems, ApJ, 468, 121

Yamada, R., Oyabu, S., Kaneda, H., et al., A Relation of the PAH 3.3 μm Feature with Star-forming Activity for Galaxies with a Wide Range of Infrared Luminosity, 2013, PASJ, 65, 103